LETTERS

Identification of a mechanism of photoprotective energy dissipation in higher plants

Alexander V. Ruban[1]*, Rudi Berera[2]*, Cristian Ilioaia[3,4], Ivo H. M. van Stokkum[2], John T. M. Kennis[2], Andrew A. Pascal[3], Herbert van Amerongen[5], Bruno Robert[3], Peter Horton[4] & Rienk van Grondelle[2]

Under conditions of excess sunlight the efficient light-harvesting antenna[1] found in the chloroplast membranes of plants is rapidly and reversibly switched into a photoprotected quenched state in which potentially harmful absorbed energy is dissipated as heat[2,3], a process measured as the non-photochemical quenching of chlorophyll fluorescence or qE. Although the biological significance of qE is established[4–6], the molecular mechanisms involved are not[7–9]. LHCII, the main light-harvesting complex, has an inbuilt capability to undergo transformation into a dissipative state by conformational change[10] and it was suggested that this provides a molecular basis for qE, but it is not known if such events occur *in vivo* or how energy is dissipated in this state. The transition into the dissipative state is associated with a twist in the configuration of the LHCII-bound carotenoid neoxanthin, identified using resonance Raman spectroscopy[11]. Applying this technique to study isolated chloroplasts and whole leaves, we show here that the same change in neoxanthin configuration occurs *in vivo*, to an extent consistent with the magnitude of energy dissipation. Femtosecond transient absorption spectroscopy[12], performed on purified LHCII in the dissipative state, shows that energy is transferred from chlorophyll *a* to a low-lying carotenoid excited state, identified as one of the two luteins (lutein 1) in LHCII. Hence, it is experimentally demonstrated that a change in conformation of LHCII occurs *in vivo*, which opens a channel for energy dissipation by transfer to a bound carotenoid. We suggest that this is the principal mechanism of photoprotection.

The twisted configuration of neoxanthin in quenched LHCII crystals and aggregates is detected by the appearance of a band at 953 cm^{-1} in the ν_4 region of the Raman spectrum[11]. Because almost all of the neoxanthin found in thylakoid membranes is bound to LHCII (ref. 13), this information can be used to probe the configuration of neoxanthin in isolated chloroplasts and whole leaves, and hence determine the presence of the quenched conformation of LHCII. *In vivo*, Raman signals arise from all the carotenoids in the thylakoid membrane, but because only neoxanthin is in a 9-*cis* conformation it exhibits fingerprint Raman bands[14], which allow its contribution to be measured; this was 50–65% of the 953 cm^{-1} signal (Supplementary Information).

Resonance Raman spectra were obtained of isolated *Arabidopsis* chloroplasts taken directly from the light (+qE) and 5 min after transfer to darkness (−qE), which resulted in collapse of the ΔpH and consequent relaxation of qE (Fig. 1a). The Raman spectra in the ν_4 region show two main bands at around 953 cm^{-1} and 964 cm^{-1}. On qE induction, there is an enhancement of the 953 cm^{-1} band relative to the 964 cm^{-1} band by 5–7%, similar to the change previously observed on an increase in quenching in isolated LHCII (ref. 10). After normalization at 1,003 cm^{-1} (the ν_3 region of the spectrum), the neoxanthin-specific spectra associated with quenching were calculated (Fig. 1b): the qE-associated spectrum shows three

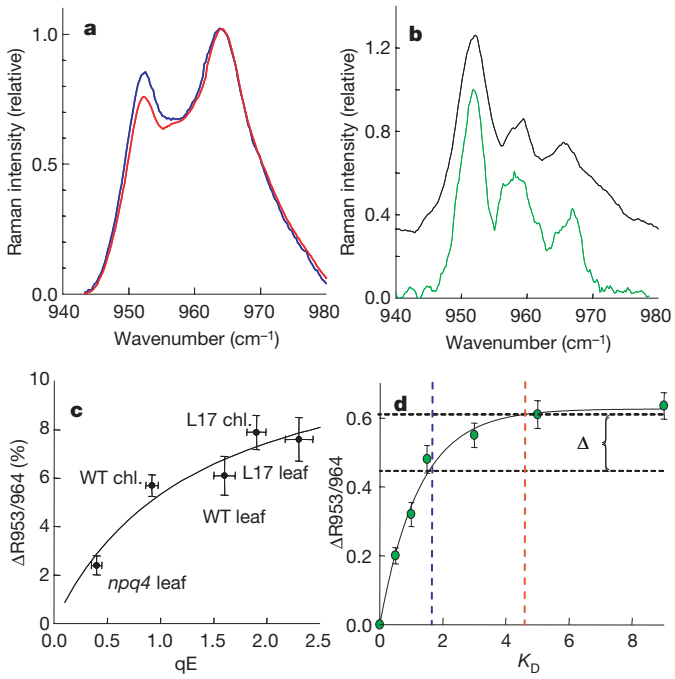

Figure 1 | Quenching-related changes in the neoxanthin region of the resonance Raman spectrum of isolated LHCII, chloroplasts and leaves. **a**, The ν_4 region of the resonance Raman spectra of wild-type chloroplasts after illumination (blue) and following a 5-min relaxation in the dark (red). **b**, Quenched−unquenched difference Raman spectra for qE (green) and for LHCII (black). For qE, the spectra were as in **a**. For LHCII unquenched and quenched, the K_d were 0 and 9, respectively (Supplementary Information). **c**, The extent of qE compared to the change in Raman intensity at 953 cm^{-1} for leaves and chloroplasts (chl.) from wild-type (WT), L17 and *npq4* plants. The data are means of *n* replicates ± s.e.m. $n = 17$ (WT chl.), 8 (L17 chl.), 3 (*npq4* leaf), 4 (WT leaf) and 3 (L17 leaf). Twenty-five spectra were recorded for each sample. The line shown is the best fit (95% confidence by *t*-test). **d**, Change in the relative Raman intensity at 953 cm^{-1} for LHCII with different extents of fluorescence quenching, K_d. For details, see text. Error bars are the calculated amplitudes of noise on the spectra.

[1]School of Biological and Chemical Sciences, Queen Mary University of London, Mile End Road, London E1 4NS, UK. [2]Department of Physics and Astronomy, Faculty of Sciences, VU University Amsterdam, De Boelelaan 1081, 1081 HV Amsterdam, The Netherlands. [3]Commissariat à l'Energie Atomique (CEA), Institut de Biologie et Technologies de Saclay (iBiTecS) and Centre National de la Recherche Scientifique (CNRS), Gif-sur-Yvette, F-91191, France. [4]Department of Molecular Biology and Biotechnology, University of Sheffield, Western Bank, Sheffield S10 2TN, UK. [5]Laboratory of Biophysics, Wageningen University, PO Box 8128, 6700 ET, Wageningen, The Netherlands.
*These authors have contributed equally to this work.

characteristic bands, which were also found in the quenched spectrum for LHCII. We then obtained further Raman spectra for both leaves and chloroplasts, not only from wild-type *Arabidopsis*, but also from the *npq4-1* mutant[15], which shows much-reduced qE, and from the PsbS-overexpressing L17 line, which shows increased qE[16]. In all cases, the extent of the enhancement of the 953 cm^{-1} band was correlated with the magnitude of qE (Fig. 1c), the maximum change being approximately 8%. The experimental design ensured that the changes in the Raman spectra were associated with qE, and did not arise from an alteration in the level of zeaxanthin: first, no epoxidation of zeaxanthin occurred during the 5-min dark relaxation period; and second, the *npq4-1* mutant showed the same level of violaxanthin de-epoxidation as the wild type and L17 mutant (data not shown). It is concluded that the formation of qE is associated with a change in configuration of neoxanthin, the same as found in quenched LHCII.

To estimate how much of a change in LHCII-bound neoxanthin would be predicted for a given change in qE, isolated LHCII was obtained in a range of oligomerization states, which cover a tenfold difference in fluorescence yield. There was a progressive increase of the intensity of the 953 cm^{-1} band on LHCII oligomerization (Supplementary Information), which correlated with the extent of fluorescence quenching (K_d) for each LHCII sample (Fig. 1d). A comparison of the *in vivo* spectrum in the unquenched state with the *in vitro* data indicate that LHCII is in a partially quenched state, corresponding to a K_d of 1.5–2.0 (blue dotted line in Fig. 1d). Hence, the change in K_d arising from qE starts from a K_d of 1.5–2.0 and reaches a maximum of 4.0–4.5 (red dotted line). Thus, we predict a maximum increase in intensity of the 953 cm^{-1} neoxanthin band of about 0.12 (approximately 20%) for an increase in K_d of 2.0 (Δ, between the two horizontal dotted lines). Taking into account the contributions of other xanthophylls (see above), the maximum predicted qE-related change in the intensity of the 953 cm^{-1} band *in vivo* would be around 10–13%—of the same order as the 8% change observed. It is concluded that under conditions of qE, a conformational change in LHCII occurs that gives rise to a significant amount of non-photochemical quenching.

We used femtosecond transient absorption spectroscopy combined with spectrally dispersed detection and global analysis[12] to determine the mechanism of quenching in isolated LHCII (and therefore in qE), specifically testing proposals that the excited chlorophyll states decay via the population of a carotenoid excited and/or charge transfer state[17–19]. Transient absorption data following a 100 fs laser pulse were obtained for the unquenched and quenched samples of LHCII, which have an approximate K_d of 0 and 9, respectively. The time traces were very different for the two samples (compare Fig. 2a and b). The spectral data at 677 nm show the initial bleaching of the chlorophyll ground state absorption, which relaxes as the excited state decays to the ground state (top). The traces describe a multiexponential process consisting of three phases: a ~1 ps component that results from excitation equilibration; a ~20 ps component assigned to singlet–singlet annihilation of chlorophyll excited states; and a slower component of ~1 ns (unquenched) and ~130 ps (quenched), which corresponds to their different chlorophyll

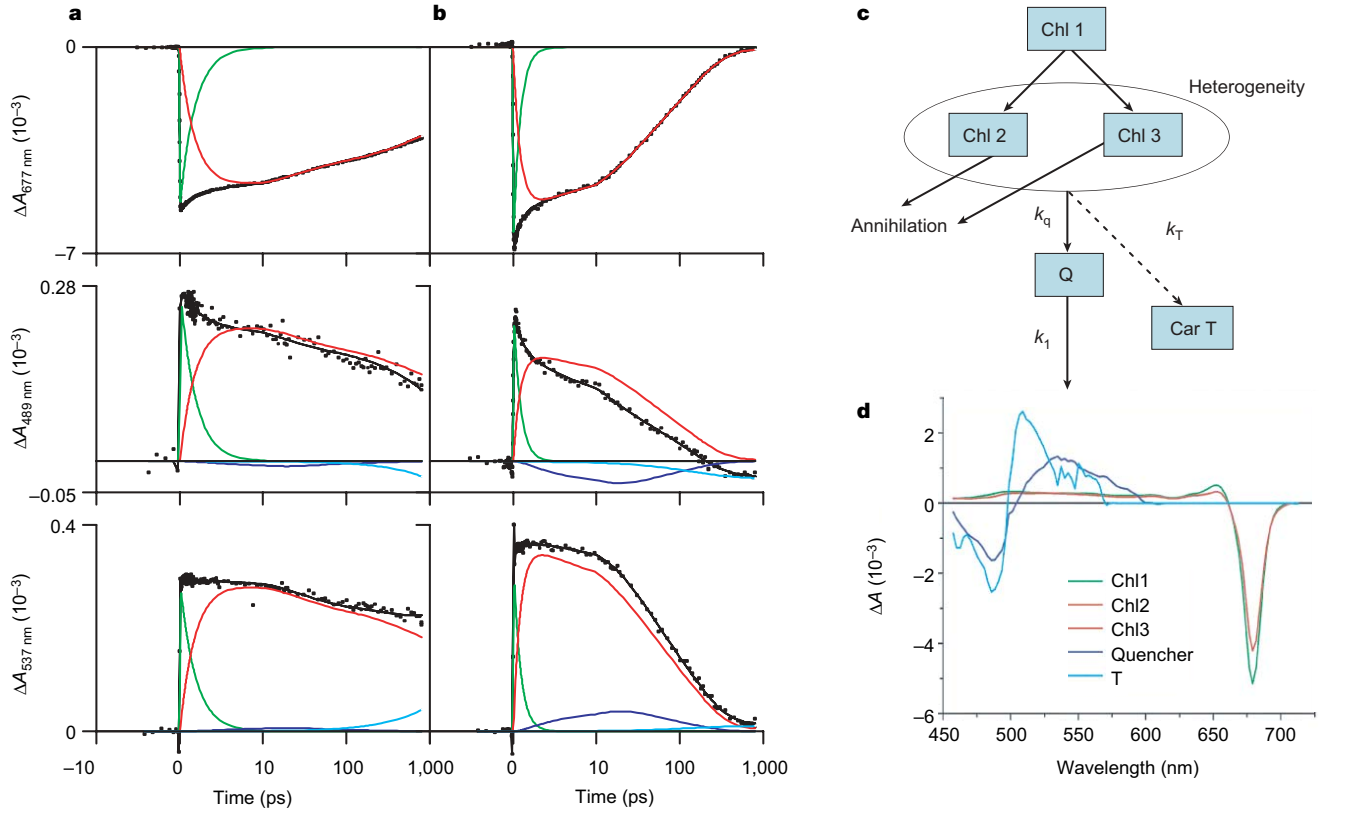

Figure 2 | Femtosecond spectroscopy of LHCII in the unquenched and quenched states. **a**, **b**, Transient absorption traces for unquenched (**a**) and quenched (**b**) LHCII at 677, 489 and 537 nm. *y* axis, absorption change, $\Delta A \times 10^{-3}$; *x* axis, linear from −10 to 10 ps and logarithmic thereafter. The curves (black) were fitted using the target analysis model (**c**, and Supplementary Information). Green, 1 ps phase due to chlorophyll excited-state relaxation; red, chlorophyll excited-state decay; blue, absorption changes due to the quencher Q; cyan, build-up of the triplet state. **c**, The model used to fit the data for quenched LHCII, with 5 compartments: at time zero the excitation resides in the first compartment (Chl 1), which relaxes on a ps timescale to Chl 2 and Chl 3. Chls 2 and 3 are introduced to account for the fraction of aggregates in which excitations are quenched by singlet–singlet annihilation (on a timescale of several tens or hundreds of ps). Both Chl 2 and Chl 3 are quenched via the quenching state Q with a rate constant k_q, and populate the triplet species Car T, with a rate constant k_T. **d**, Species-associated difference spectra (SADS). Green, the initial excited state (Chl 1); red, Chl 2 and 3; dark blue, the quenching state Q; cyan, Car T.

excited-state lifetimes. The traces at 489 nm (middle) and 537 nm (bottom)—wavelengths that are in the regions of carotenoid ground-state bleach and excited-state absorption, respectively—are only slightly different for the unquenched sample. However, for the quenched sample these traces differ markedly: the 489 nm trace shows decay on the 10–20 ps timescale that is absent in the 537 nm trace. In contrast, the decay at 537 nm is slower on the 10–20 ps timescale when compared to the chlorophyll decay at 677 nm. These differences suggest that in the quenched sample, concomitant with the decay of the chlorophyll excited states, another species is transiently populated, which we will identify as a carotenoid S_1 state—a low-lying optically forbidden excited state. In samples with a K_d of approximately 2, the same carotenoid feature was observed, but to a lesser extent (Supplementary Information). Extensive probing of the 900–1,000 nm region in the same time window did not reveal any absorption changes that could be ascribed to a carotenoid radical (Supplementary Information).

To identify the spectrum of the quenching state, a target analysis was applied to the time-resolved data[12] (Fig. 2c, d). The results from the target analysis demonstrate the essential role of the carotenoid S_1 state in the quenching process. The chlorophyll spectrum shows the bleach of the chlorophyll Q_y state in the 675 nm region, a dip around 615 nm, corresponding to the bleach of the chlorophyll Q_x state, and a region of almost flat excited-state absorption. The cyan spectrum corresponds to the long-lived carotenoid triplet state. The spectrum of the quencher (blue line) reveals the following features: excited state absorption between 505 and 600 nm, corresponding to the carotenoid $S_1 \rightarrow S_n$ transition; and ground-state bleach below 505 nm, corresponding to the bleach of the carotenoid $S_0 \rightarrow S_2$ transition. With the same model applied to the unquenched sample the quenching state remained almost unpopulated. The target analysis yielded an excellent fit to the transient absorption traces (Fig. 2a, b). Most importantly, in quenched LHCII, there is a significant deviation between the chlorophyll excited-state decay kinetics and the traces measured at 489 and 537 nm, owing to population of the carotenoid S_1 state (blue lines); however, in the unquenched sample, these kinetics are the same.

The spectral evolution in the carotenoid absorption region is strongly reminiscent of that observed in artificial carotenoid—phthalocyanine dyads, in which it was demonstrated that quenching occurred via the population of the carotenoid S_1 state[19]. Thus, in the same way, our data provide unequivocal evidence for the population of a carotenoid excited state that is concomitant with the quenching of chlorophyll excited states in aggregates of LHCII, strongly pointing to chlorophyll *a*–carotenoid energy transfer as the quenching mechanism. The samples used here contain only trace levels of violaxanthin (and no zeaxanthin), so lutein or neoxanthin must be responsible for the absorption changes associated with quenching. A comparison of the bleach of the quenching state with the bleach of the carotenoid triplet state shows that their corresponding negative-peak positions coincide. The maximum bleach in the carotenoid triplet spectrum corresponds to lutein 1 (ref. 20). Consequently, lutein 1 is also likely to be the quencher. Lutein 1 is found in an LHCII domain containing chlorophyll *a* 610, chlorophyll *a* 611 and chlorophyll *a* 612 (ref. 21), where the excitation has the highest possibility to be localized, and therefore it is the obvious site for quenching[22].

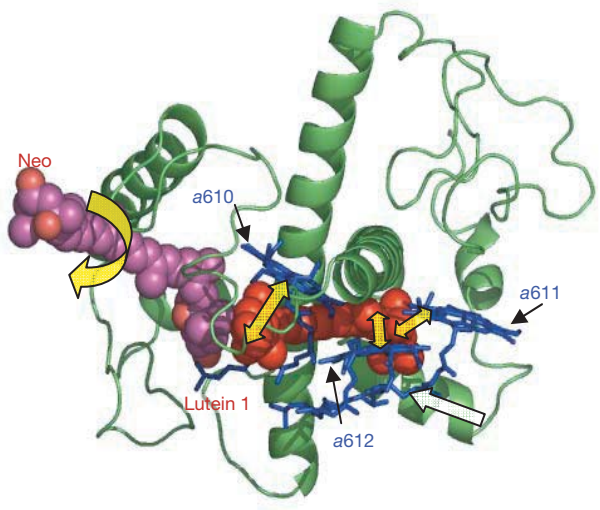

Figure 3 | Model illustrating the molecular mechanism of qE. Structural model of an LHCII monomer[21] showing the key pigments involved in the establishment of qE. Lutein 1 (red) is closely associated with chlorin rings of chlorophyll *a* 610, 611 and 612 (blue, small black arrows). Curved broad yellow arrow, the configurational twist of the neoxanthin (Neo) molecule (pink); white broad arrow, the putative movement of lutein 1 towards the chlorophyll cluster (broad yellow arrows).

Studies using isolated LHCII and related antenna complexes have provided important insights into the mechanism of qE[2,23,24]. Most importantly, it was shown that crystallized LHCII is in a quenched state[10], demonstrating that energy dissipation was an intrinsic feature of each LHCII molecule that is brought about by specific configurations of the chlorophylls and xanthophylls bound to the complex, and proving that LHCII can exist in different conformational states that have differing capacities for energy dissipation. However, there was no direct proof that the proposed conformational changes occur *in vivo*; such proof has now been provided from Raman spectroscopy of chloroplasts and leaves in different qE states. The same twisted configuration in neoxanthin was found in both quenched LHCII *in vitro* and in thylakoid membranes *in vivo* under conditions in which the rapidly reversible, ΔpH-dependent (qE) form of non-photochemical quenching is present. We conclude that quenching occurs under these conditions by the same process as *in vitro*. Therefore we re-affirm a model in which qE is initiated by a conformational change in LHCII, which is induced by the light-dependent ΔpH (ref. 2). We propose that this change in conformation gives rise to an increase in the rate of energy transfer to lutein 1 and, consequently, to energy dissipation (Fig. 3). LHCII aggregation has previously been associated with a conformational change in the lutein 1 domain[25]. Moreover, from a comparison of lutein 1 and lutein 2 in the crystal structure, it has been speculated how a change in the configuration of lutein 1 would bring it closer to chlorophyll *a* 612 (ref. 26), providing the key step in the switching on of quenching. This idea provides an explanation of the link between the observed changes in protein conformation and fluorescence quenching.

Although this model can fully account for qE both qualitatively and quantitatively, qE may be a heterogeneous process of which quenching by lutein 1 in LHCII is only a part. The formation of a radical state of zeaxanthin has been correlated with qE *in vivo*, suggesting that it is either the quencher itself or its formation is closely associated with the quenching process[7]. Although we did not detect the presence of a charge-separated state involving a carotenoid radical in quenched LHCII aggregates, the LHCII samples used here do not contain any zeaxanthin. Similarly, our data do not exclude the possibility that quenching also occurs in the minor antenna complexes, CP24, CP26 and CP29, which have been reported to bind zeaxanthin at sites occupied by lutein in the major LHCII (ref. 24). Further work is needed to establish the relationship between different xanthophyll excited states and radical states *in vivo*, and the contributions they make not only to qE but to other more sustained energy dissipation states that can arise under certain extreme conditions of plant stress[27] and that seem to involve formation of LHCII aggregates similar to those used here[28]. Clearly, however, both the conformation of antenna complexes and the specific xanthophylls they bind play vital parts in tuning the function of the light-harvesting antenna to physiological need.

METHODS SUMMARY

LHCII trimers were prepared from spinach photosystem-II-enriched particles by isoelectric focusing, followed by sucrose gradient centrifugation[29]. Oligomeric LHCII was obtained by incubation with SM-2 Absorbent (Bio-Rad). Chloroplasts from *Arabidopsis thaliana* were isolated and assayed as described previously[30]. Room temperature fluorescence data (qE, K_d) are presented in the form F(unquenched)−F(quenched)/F(quenched). Raman measurements were obtained at 77 K using 488 nm excitation[10,14], and the presented spectra normalized to 964 cm^{-1} unless stated otherwise. Transient absorption spectroscopy used 675 nm 100 fs laser pulses, with a repetition rate of 40 kHz and energy per pulse of about 10 nJ. The data were subjected to global and target analysis[12].

Full Methods and any associated references are available in the online version of the paper at www.nature.com/nature.

Received 30 April; accepted 14 September 2007.

1. van Grondelle, R. *et al.* Energy transfer and trapping in photosynthesis. *Biochim. Biophys. Acta* **1187,** 1–65 (1994).
2. Horton, P., Ruban, A. V. & Walters, R. G. Regulation of light harvesting in green plants. *Annu. Rev. Plant Physiol. Plant Mol. Biol.* **47,** 655–684 (1996).
3. Niyogi, K. K. Photoprotection revisited. *Annu. Rev. Plant Physiol. Plant Mol. Biol.* **50,** 333–359 (1999).
4. Demmig-Adams, B. & Adams, W. W. III. Antioxidants in photosynthesis and human nutrition. *Science* **298,** 2149–2153 (2002).
5. Horton, P. & Ruban, A. V. Molecular design of the photosystem II light harvesting antenna: photosynthesis and photoprotection. *J. Exp. Bot.* **56,** 365–373 (2005).
6. Külheim, C., Ågren, J. & Jansson, S. Rapid regulation of light harvesting and plant fitness in the field. *Science* **297,** 91–93 (2002).
7. Holt, N. E. *et al.* Carotenoid cation formation and the regulation of photosynthetic light harvesting. *Science* **307,** 433–436 (2005).
8. Standfuss, J. *et al.* Mechanisms of photoprotection and nonphotochemical quenching in pea light-harvesting complex at 2.5 Å resolution. *EMBO J.* **24,** 919–928 (2005).
9. Horton, P., Wentworth, M. & Ruban, A. V. Control of the light harvesting function of chloroplast membranes: the LHCII-aggregation model for non-photochemical quenching. *FEBS Lett.* **579,** 4201–4206 (2005).
10. Pascal, A. A. *et al.* Molecular basis of photoprotection and control of photosynthetic light-harvesting. *Nature* **436,** 134–137 (2005).
11. Robert, B. *et al.* Insights into the molecular dynamics of the plant light harvesting proteins *in vivo*. *Trends Plant Sci.* **9,** 385–390 (2004).
12. van Stokkum, I. H. M., Larsen, D. S. & van Grondelle, R. Global and target analysis of time-resolved spectra. *Biochim. Biophys. Acta* **1657,** 82–104 (2004).
13. Bassi, R., Pineau, B., Dainese, P. & Marquardt, J. Carotenoid-binding proteins of photosystem II. *Eur. J. Biochem.* **212,** 297–303 (1993).
14. Ruban, A. V., Pascal, A. A. & Robert, B. Xanthophylls of the major photosynthetic light-harvesting complex of plants: identification, conformation and dynamics. *FEBS Lett.* **477,** 181–185 (2000).
15. Li, X. P. *et al.* A pigment-binding protein essential for regulation of photosynthetic light harvesting. *Nature* **403,** 391–395 (2000).
16. Li, X. P. *et al.* PsbS-dependent enhancement of feedback de-excitation protects photosystem II from photoinhibition. *Proc. Natl Acad. Sci. USA* **99,** 15222–15227 (2002).
17. Frank, H. A. *et al.* Mechanism of nonphotochemical quenching in green plants: Energies of the lowest excited singlet states of violaxanthin and zeaxanthin. *Biochemistry* **39,** 2831–2837 (2000).
18. Ma, Y. Z. *et al.* Evidence for direct carotenoid involvement in the regulation of photosynthetic light harvesting. *Proc. Natl Acad. Sci. USA* **100,** 4377–4382 (2003).
19. Berera, R. *et al.* A simple artificial light-harvesting dyad as a model for excess energy dissipation in oxygenic photosynthesis. *Proc. Natl Acad. Sci. USA* **103,** 5343–5348 (2006).
20. Lampoura, S. S. *et al.* Aggregation of LHCII leads to a redistribution of the triplets over the central xanthophylls in LHCII. *Biochemistry* **41,** 9139–9144 (2002).
21. Liu, Z. *et al.* Crystal structure of spinach major light-harvesting complex at 2.72 Å resolution. *Nature* **428,** 287–292 (2004).
22. van Grondelle, R. & Novoderezhkin, V. I. Energy transfer in photosynthesis: experimental insights and quantitative models. *Phys. Chem. Chem. Phys.* **8,** 793–807 (2006).
23. Moya, I. *et al.* Time-resolved fluorescence analysis of the photosystem II antenna proteins in detergent micelles and liposomes. *Biochemistry* **40,** 12552–12561 (2001).
24. Morosinotto, T., Baronio, R. & Bassi, R. Dynamics of chromophore binding to Lhc proteins *in vivo* and *in vitro* during operation of the xanthophyll cycle. *J. Biol. Chem.* **277,** 36913–36920 (2002).
25. Wentworth, M., Ruban, A. V. & Horton, P. Thermodynamic investigation into the mechanism of the chlorophyll fluorescence quenching in isolated photosystem II light harvesting complexes. *J. Biol. Chem.* **278,** 21845–21850 (2003).
26. Yan, H. *et al.* Two lutein molecules in LHCII have different configurations and functions: insights into the molecular mechanism of thermal dissipation in plants. *Biochem. Biophys. Res. Commun.* **355,** 457–463 (2007).
27. Demmig-Adams, B. & Adams, W. W. III. Photoprotection in an ecological context: the remarkable complexity of thermal energy dissipation. *New Phytol.* **172,** 11–21 (2006).
28. Tang, Y. *et al.* Heat stress induces aggregation of the light harvesting complex of photosystem II in spinach plants. *Plant Physiol.* **143,** 629–638 (2007).
29. Ruban, A. V. *et al.* Determination of the stoichiometry and strength of binding of xanthophylls to the photosystem II light harvesting complexes. *J. Biol. Chem.* **274,** 10458–10465 (1999).
30. Crouchman, S., Ruban, A. V. & Horton, P. PsbS enhances nonphotochemical fluorescence quenching in the absence of zeaxanthin. *FEBS Lett.* **580,** 2053–2058 (2006).

Supplementary Information is linked to the online version of the paper at www.nature.com/nature.

Acknowledgements This work was supported by grants from: UK Biotechnology and Biological Sciences Research Council (P.H., A.V.R.); the Netherlands Organization for Scientific Research via the Foundation of Earth and Life Sciences (R.v.G., H.v.A., J.T.M.K., R.B.) and a VIDI Fellowship (J.T.M.K); Laserlab Europe; ANR (program caroprotect) (A.A.P., B.R.); and the INTRO2 EU FP6 Marie Curie Research Training Network. We thank K. K. Niyogi for the gift of seeds of the L17 *Arabidopsis* line.

Author Information Reprints and permissions information is available at www.nature.com/reprints. Correspondence and requests for materials should be addressed to P.H. (p.horton@sheffield.ac.uk), B.R. (bruno.robert@cea.fr) or R.v.G. (rienk@few.vu.nl).

METHODS

LHCII preparation and analysis. LHCII trimers prepared from spinach photosystem II particles were incubated at a chlorophyll concentration of 1 mg ml^{-1} in a 2 ml volume in a 1 cm × 1 cm cuvette in the presence of 0.01% *n*-dodecyl β-D-maltoside. Biobeads (300 mg; SM-2 Absorbent) were added. Chlorophyll fluorescence was monitored with a Walz MiniPam fluorimeter. The decline in fluorescence started after approximately 10 min and quenching reached a K_d of around 8–10 after 40 min. For Raman experiments, samples were taken at appropriate K_d values and immediately frozen in liquid nitrogen in the Raman sample holders. For transient absorption experiments the concentration of LHCII was adjusted to give $A_{670\,nm}$ 0.3–0.5 at the chlorophyll Qy maximum.

Chloroplasts and leaves. Chloroplasts were prepared from dark-adapted *Arabidopsis* plants. Chloroplasts were ruptured by brief osmotic shock in 5 mM $MgCl_2$ and measured in a reaction medium containing 0.33 M sorbitol, 20 mM HEPES, pH 7.8, 5 mM $MgCl_2$ and 0.1 mM methyl viologen. The chlorophyll concentration was 20 μM. Chlorophyll fluorescence analysis was carried out using a Walz PAM101 fluorimeter. A light saturation pulse was given at the ends of the light and dark periods to give the Fm' and Fm levels respectively. qE was calculated as Fm–Fm'/Fm'. Chloroplasts were measured in a 1 cm × 1 cm cuvette. Samples taken after 5 min illumination (1,500 μmol m^{-2} s^{-1} light) and following 5 min dark relaxation were transferred to the Raman sample holder and immediately frozen with liquid nitrogen. Detached, dark-adapted *Arabidopsis* leaves were placed in the Raman sample holder and chlorophyll fluorescence analysis was carried out using the same protocol as for chloroplasts, and similarly frozen, immediately after the light or dark treatment.

Pigment analysis. Pigment compositions of LHCII and chloroplasts were determined by HPLC using a reverse phase C18 column (Merck LiChrospher 100 RP-18) and Dionex chromatography system. The solvent system was (solvent A, 87% acetonitrile, 10% methanol, 3% 0.1 M TRIS, pH 8; solvent B, 80% methanol, 20% hexane). The gradient from solvent A to solvent B was run from 9 to 12.5 min at a flow rate of 1 ml min^{-1}. Each peak was integrated at its optimum absorbance and analysed using Dionex Chromeleon software. The analysis showed that the LHCII samples contained only trace amounts of violaxanthin (0.3 ± 0.2% of the total carotenoid) and no detectable antheraxanthin or zeaxanthin.

Transient absorption spectroscopy. Transient absorption spectroscopy used femtosecond pulses obtained from a titanium:sapphire oscillator-regenerative amplifier (coherent MIRA seed and RegA). The repetition rate was 40 kHz and the initial pulse ~60 fs at 800 nm. The beam was split into two, one of which (the probe beam) was focused on a CaF_2 plate to generate a white-light continuum. The other beam was used to pump an optical parametric amplifier to obtain the pump beam at 675 nm (~100 fs). The energy per pulse was about 10 nJ. The polarization between the pump and probe beams was set at the magic angle. High repetition rate, single-shot multi-channel detection and rejection of outliers improved the signal-to-noise ratio by about a factor of ten (compared to a standard pump–probe experiment).